The 22nd European symposium on Ultrasound Contrast Imaging, 19-20 January 2017, Rotterdam-The Nederland's, An ICUS Conference

Numerical study on the static response of contrast agent microbubbles

Alkmini D. Lytra & Nikos A. Pelekasis
Lab. of Fluid Mechanics & Turbomachinery, Dep. of Mechanical Engineering, University of Thessaly, Greece
pel@uth.gr, http://contrast-aristeia.mie.uth.gr/

Scope & Abstract

There are two major families of coating materials that are usually employed in medical applications: polymeric and lipids. Polymeric shells are characterized by higher area dilatation modulus and shell thickness in comparison with shells covered with lipids. The latter are softer and exhibit significant deformations when subjected to forces as low as several nN. The present study presents calculations of the static deformation of a coated microbubble that is compressed by a rigid surface, in order to assist the interpretation of Atomic Force Microscopy measurements conducted to provide estimates of the shell elastic properties.

- A contact model is proposed for microbubbles covered with a polymeric shell based on the classic shell mechanics[1].
- For microbubbles with a lipid shell a model that accounts for intermolecular forces is employed, by introducing an adhesive potential[2] which describes the disjoining pressure between the shell and the AFM cantilever. Thus, an additional resistance to the cantilever's advancement is introduced in order to account for the ultrathin water layer that occupies the space between the shell and cantilever, as a result of their hydrophilic nature, and resists thinning as the external pressure increases.
- In both models axisymmetry is assumed with respect to the vertical axis and symmetry in the equator. The resistance to gas compression is accounted for as well as the non-linearity of the constitutive law for the elastic shell[3].

Theoretical Modelling

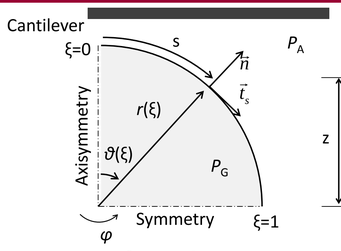

Reference State

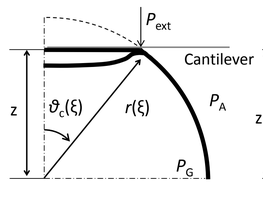

Classic Contact Problem

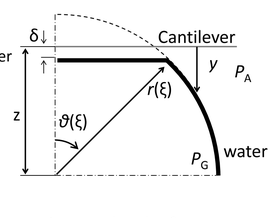

Intermolecular forces - contact model

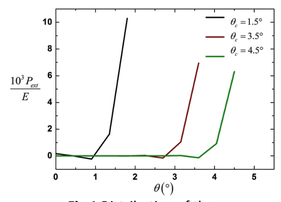

Fig.1 Distribution of the contact pressure.

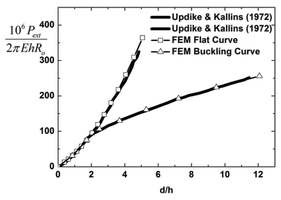

Fig.2 Validation of the classic contact model[4].

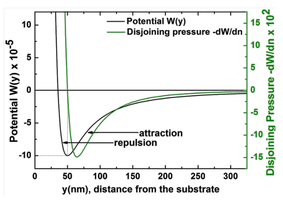

Fig.3 Distribution of the disjoining pressure & Adhesive Potential.

Normal Force Balance $\vec{n}: P_G - P_A = k_s\tau_{ss} + k_\varphi\tau_{\varphi\varphi} + (\gamma_{BW} + W)\vec{\nabla}_s\cdot\vec{n} - \frac{1}{\sigma}\frac{\partial(\sigma q)}{\partial s} + \Pi$

Tangential Force Balance $\vec{t}_s: -\left[\frac{\partial\tau_{ss}}{\partial s} + \frac{1}{\sigma}\frac{\partial\sigma}{\partial s}(\tau_{ss} - \tau_{\varphi\varphi}) + k_s q\right] = 0,$

$\vec{q} = \vec{\nabla}_s\cdot\underline{m}\cdot(\underline{\underline{I}} - \vec{n}\vec{n}),\ \sigma = r\sin\theta$

Isothermal Gas Compression: $P_G V_f^\gamma = P_A V_i^\gamma$

Elastic Energy Functions:

$$(\text{Hook})\, w^{HK} = \frac{G_s}{4(1-\nu)}\left[(\lambda_s^2-1)^2 + 2\nu(\lambda_s^2-1)(\lambda_\varphi^2-1) + (\lambda_\varphi^2-1)^2\right],$$

$$(\text{Mooney-Rivlin})\, w^{MR} = w(I_1,I_2) = \frac{G_{MR}}{2}\left[(1-b)\left(I_1 + 2 + \frac{1}{I_2+1}\right) + b\left(\frac{I_1+2}{I_2+1} + I_2 + 1\right)\right]$$

Bending Moments: $m_{ii} = \frac{k_b}{\lambda_j}(K_i + \nu K_j),\ i,j \to s,\varphi$ direction,

I_1, I_2 Invariants of Green-Lagrange deformation tensor

$$G_s = \frac{\chi}{2(1+\nu)},\ G_{MR} = \frac{\chi}{3},\ \chi = Eh, k_b = \frac{Eh^3}{12(1-\nu^2)}$$

$$\Pi = \begin{cases} P_{ext}, & \text{Unknown line load, classic contact model} \\ -\frac{\partial W}{\partial n} = -\frac{\partial W}{\partial y}\frac{\partial y}{\partial n}, & \text{Disjoining pressure, Intermolecular forces model} \end{cases}$$

$$W = W(y) = W_0\left[\left(\frac{\delta_A}{y}\right)^4 - 4\left(\frac{\delta_A}{y}\right)^2\right]$$

Kinematic Condition: $\frac{d(r\cos\theta)}{d\xi} = 0$, at $\theta=\theta_c$ in classic contact model

BC: $r_\xi(\xi = 0 \text{ and } 1) = \theta_{\xi\xi}(\xi = 0 \text{ and } 1) = 0,\ \theta(\xi=0) = 0,\ \theta(\xi=1) = \frac{\pi}{2}$

The problem formulation is rendered dimensionless by introducing the characteristic length scale, R_o. Then the solution depends mainly on three dimensionless parameters,

$\hat{k}_b, \hat{P}_A, \hat{\gamma}_{BW}$ and $\hat{W}$: $\hat{r} = \frac{r}{R_o};\ \hat{k}_b = \frac{k_b}{\chi R_o^2};\ \hat{P}_A = \frac{P_A R_o}{\chi};\ \hat{\gamma}_{BW} = \frac{\gamma_{BW}}{\chi};\ \hat{W} = \frac{W}{\chi};\ \hat{\chi} = 1.$

Total force on the shell due to intemolecular forces: $\vec{F} = -\int_A\left(\frac{\partial W}{\partial n} + 2k_m W\right)dA\vec{e}_z$

The above set of equations is solved via **Finite Element Method** by using the B-cubic Splines as basis function and performing **simple** and **arc-length continuation**. The **Fortran** code has been **validated** with the analytical solution of Updike & Kallins[4] and the critical buckling load, when the shell is compressed by a uniform pressure load[5].

Results

Microbubbles covered with polymer

Asymptotic Analysis-Shell properties estimation

The force-deformation (f-d) curves obtained with an AFM[6] for microbubbles covered with polymer exhibit initially a linear regime followed by a non-linear curved downwards. This behavior conforms with the classic transition from the linear, Reissner, to the nonlinear, Pogorelov, regimes in the f-d curves. Employing analytical expressions from Reissner and Pogorelov theory[1] the shell thickness (h) and Young modulus (E) can be estimated with excellent agreement[7] with the experimentally obtained values, Fig. 4 and Table 1.

- Reissner's Equation: $F = \frac{4}{\sqrt{3(1-\nu^2)}}\frac{Eh^2}{R_o}\Delta$ or $F = 8\sqrt{\chi k_b}\frac{\Delta}{R_o}$
- Pogorelov's Equation: $F = \left[\frac{3.56E^2h^5}{(1-\nu^2)^2 R_o^2}\Delta\right]^{0.5}$

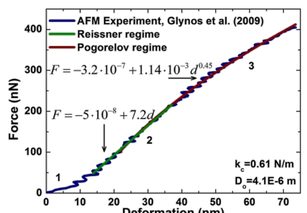

Fig.4 Experimental f-d curve with fitting of Reissner & Pogorelov eq.

Shell Diameter, D_o [μm]	Experimental Values[6] E [GPa]	h [nm]	Asymptotic Estimation[7] E [GPa]	h [nm]
2.6	10-16	20	8.5	25
4.1	2.5-6	31	6.1	31
3.1	6-10	23	3.4	35
4.0	2.5-6	30	4.7	30
5.5	1-3	41	1.7	47

Table 1 Comparison of the experimental and calculated via the Reissner-Pogorelov eq. values of Young modulus and shell thickness.

Numerical Simulation-Classic contact formulation

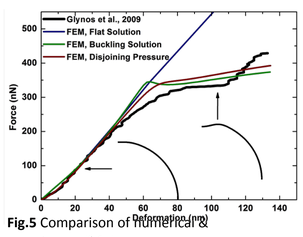

Fig.5 Comparison of numerical & experimental[6] f-d curves

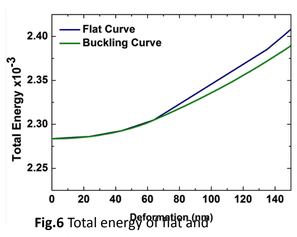

Fig.6 Total energy of flat and buckling solutions

Simulation parameters

$R_o = 2.0\ \mu m, E = 4.7\ GPa, h = 30\ nm, \nu = 0.42,$
$u = -1.25\cdot10^{-3}\ \mu m, \gamma_{BW} = 0.051\ N/m,$
$\gamma = 1.07$, Hook's law and 400 B-Cubic Splines.

$\hat{k}_b = 2.3\cdot10^{-5};\ \hat{P}_A = 1.43\cdot10^{-3};\ \hat{\gamma}_{BW} = 3.6\cdot10^{-4};\ \hat{W} = 7.1\cdot10^{-6}$

The FEM f-d curves for polymeric shells with the classic contact model exhibit the same regimes, characterized by shapes that are flat or bended in the pole region, Fig 5. The linear regime loses stability after the buckling point due to excessive compression and the solution in this regime is characterized by an additional unstable eigenvalue. This behavior is in agreement with the total energy of each branch, which is higher in the flat solution after the buckling point (d=60 nm), Fig. 6.

Microbubbles covered with lipid monolayer

Numerical Simulation-Intermolecular forces model

The f-d curve obtained with the intermolecular forces model (red curve Fig. 7) for a microbubble covered with lipid is directly compared against the one obtained with the AFM[8] (black curve Fig.7). The two curves coincide with satisfactory agreement up to deformation of 300 nm and shell buckling is not detected, Fig. 8. This behavior conforms well with the Reissner response pattern. Due to the relatively small bending to dilatational stiffness ratio, and the stabilizing effect of adhesion onto the cantilever, the Pogorelov regime is bypassed and the Reissner curve persists until relatively large forces. Repeating the calculation employing the Reissner model[4] produces almost the same response, (green curve, Fig 7).

The variation of the disjoining pressure in the contact area between the AFM and the shell indicates that the liquid film height in not constant, Fig.9 and the its maximum value around the end of contact area is in agreement with the classic contact model.

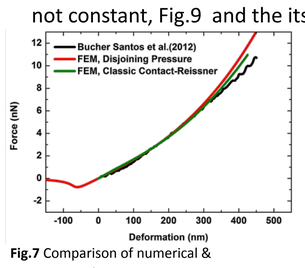

Fig.7 Comparison of numerical & experimental[8] f-d curves.

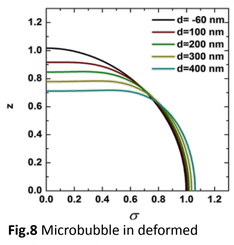

Fig.8 Microbubble in deformed configuration for selected values of deformation.

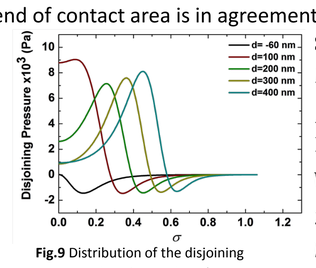

Fig.9 Distribution of the disjoining pressure along the shell surface.

Simulation parameters
$R_o = 1.5\ \mu m,$
$\chi = 0.05\ N/m, k_b = 3\cdot10^{-16}\ Nm, \nu = 0.5,$
Mooney-Rivlin law, b=1
$W_o = 10^{-4}\ N/m, \delta_A = 50\ nm, \gamma_{BW} = 0\ N/m,$
$\gamma = 1.07$ and 400 B-Cubic Splines.
$\hat{k}_b = 2.7\cdot10^{-3};\ \hat{P}_A = 3;\ \hat{W}_{BW} = 2\cdot10^{-3}$

Parametric Study

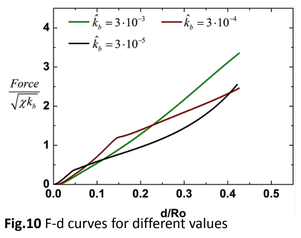

Fig.10 F-d curves for different values of dimensionless bending modulus.

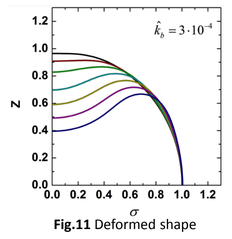

Fig.11 Deformed shape with buckling.

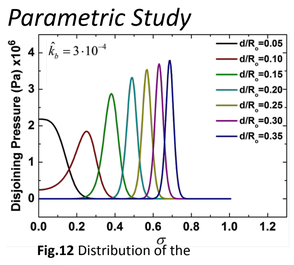

Fig.12 Distribution of the disjoining pressure.

Effect of dimensionless bending modulus $\hat{k}_b$

- Smaller values of dimensionless bending modulus lead to buckling of the shell.
- The buckling point is shifted to higher values of deformation as $\hat{k}_b$ increases.
- The disjoining pressure is concentrated in the dimple of the buckling.
- Simulations for the parameter range relevant to polymeric shells reproduce the results of the classic contact model, red curve Fig. 5.

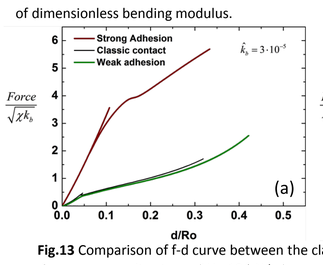

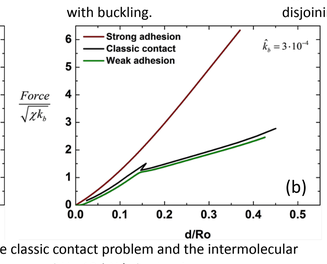

Fig.13 Comparison of f-d curve between the classic contact problem and the intermolecular forces model with strong (W_o=10^{-1} N/m) and weak (W_o=10^{-4} N/m) adhesion (a) $\hat{k}_b = 3\cdot10^{-5}$, (b) $\hat{k}_b = 3\cdot10^{-4}$.

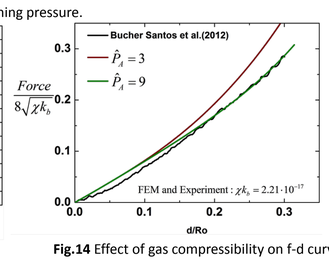

Fig.14 Effect of gas compressibility on f-d curve.

Effect of gas compression $\hat{P}_A$

- The FEM f-d curve is initially linear, recovering the Reissner regime.
- In higher deformations an almost quadratic response ($\Delta^{2.5}$) is recovered.
- Gas compressibility determines the rigidity of the coated microbubble.

Effect of adhesive energy W_o

- When the adhesion (W_o) is high, buckling is postponed (Fig. 13a) or even bypassed (Fig. 13b).
- The weak adhesion gives the same results with the classic contact model.
- Preliminary parameters estimation based on this procedure provides reasonable estimates of the bending ($k_b = 4.42\cdot10^{-16}\ Nm$) and area dilatation ($\chi = 0.05\,N/m$) moduli.

Conclusions

- The classic contact model is a simple and sufficient theoretical tool to investigate the response of polymeric coatings.
- The static response of such microbubbles is obtained via FEM simulations based on the above model, in the form of two intersecting solution braches: the flat and the buckling, with the former losing stability at the buckling point.
- The elastic properties of microbubbles covered with thin polymeric shells can be estimated from AFM[6] measurements by the transition from the flat (Reissner) to the buckled (Pogorelov) branch.
- The intermolecular forces model is a novel tool that recovers the experimental f-d curve for microbubbles covered with either polymeric or phospholipid monolayer shells.
- For the experiments[8] with lipid monolayer shells buckling in not detected – The static response initially follows the linear Reissner solution where bending stiffness dominates.
- The parametric analysis shows that the dimensionless bending modulus controls the buckling point, but in case of strong adhesion buckling is postponed to higher values of force and deformation or bypassed.
- Beyond a certain level of deformation resistance to compression dominates rigidity and an almost quadratic ($\Delta^{2.5}$) response pattern is recovered.
- The elastic properties, namely area dilatation and bending modulus, of phospholipid shells can also be estimated from AFM[8] measurements by the transition from the bending stiffness (Reissner) regime to gas compressibility dominated regime.
- Based on the above analysis, it can be concluded that microbubbles covered with lipid monolayer behave like viscoelastic solids.

Selected References

1. Landau, L.D., et al., *Theory of Elasticity*. 1986: Butterworth-Heinemann.
2. Blount, M.J., M.J. Miksis, and S.H. Davis, *The equilibria of vesicles adhered to substrates by short-ranged potentials.* Proc. R Soc. A, 2013. **469**(2153).
3. Barthes-Biesel, D., A. Diaz, and E. Dhenin, *Effect of constitutive laws for two-dimensional membranes on flow-induced capsule deformation.* JFM, 2002. **460**: p. 211-222.
4. Updike, D.P. and A. Kalnins, *Axisymmetric Postbuckling and Nonsymmetric Buckling of a Spherical Shell Compressed Between Rigid Plates.* J. Appl. Mech. T ASME, 1972. **39**(1): p. 172-178.
5. Lytra, A. & N. Pelekasis, *Static response and stability of coated microbubbles—multiplicity of solutions and parameter estimation.* Fluid Dyn. Res., 2014. **46**(4): p. 041422.
6. Glynos, E., et al., *Nanomechanics of Biocompatible Hollow Thin-Shell Polymer Microspheres.* Langmuir, 2009. **25**(13): p. 7514-7522.
7. Lytra, A., N. Pelekasis, V. Sboros, E. Glynos, V. Koutsos, *Static Response of Coated Microbubbles: Modeling Simulations and Parameter Estimation.* Procedia IUTAM, 2015. **16**: p. 123-133.
8. Buchner Santos, E., et al., *Nanomechanical Properties of Phospholipid Microbubbles.* Langmuir, 2012. **28**(13): p. 5753-5760.

Acknowledgments

This work was performed in the framework of the operational program: «Education and lifelong learning» - «**Aristeia I**» and was cofounded by the European Union (European Social Fund) and national resources.
The authors wish also to thank Dr. V. Koutsos, Dr. V. Sboros and Dr. E. Glynos for fruitful discussions on the AFM and for kindly providing the experimental (AFM) data.

European Union
European Social Fund
OPERATIONAL PROGRAMME EDUCATION AND LIFELONG LEARNING
Investing in knowledge society
MINISTRY OF EDUCATION & RELIGIOUS AFFAIRS
MANAGING AUTHORITY
NSRF 2007-2013
programs for development
EUROPEAN SOCIAL FUND
Co-financed by Greece and the European Union